Operation and Performance of Belle II Aerogel RICH Counter

Shohei Nishida

High Energy Accelerator Research Organization (KEK), Tsukuba, Ibaraki, 305-0801, Japan

E-mail: shohei.nishida@kek.jp

Abstract. The Belle II experiment at the SuperKEKB aims at collecting 50 times more data than its predecessor Belle. One of the key components in the experiment is the particle identification (PID), especially the separation of kaons and pions. In the Belle II spectrometer, a proximity focusing ring imaging Cherenkov detector using aerogel as a radiator (ARICH) is equipped for the PID at the forward endcap. In this counter, a total of 420 of hybrid avalanche photo-detectors (HAPDs) with 144 channels are used as position-sensitive photon detectors that work inside a 1.5 T magnetic field. Belle II started the physics run with full detectors from 2019. We report on the operation of ARICH, including the fraction of dead channels, stability of HAPDs, and encountered problems. We also report the PID performance of ARICH estimated with using $D^{*+} \to D^0\pi^+_{\rm slow}$, $D^0 \to K^-\pi^+$ control sample with the initial data.

1. Introduction

Belle II [1] is a flavor physics experiment at KEK with the SuperKEKB asymmetric e^+e^- collider (4 GeV on 7 GeV) [2]. Belle II plans to accumulate 50 ab^{-1} integrated luminosity in 10-year operation, which is 50 times larger than the previous Belle experiment. Particle identification (PID) especially the separation of pions and kaons[1] plays an important role in such a flavor physics experiment. In the Belle II spectrometer, a proximity focusing ring imaging Cherenkov detector using aerogel as a radiator (ARICH) is equipped for the PID at the forward endcap. Momenta of particles originated from B mesons produced at SuperKEKB are below 4 GeV.

2. Overview of the ARICH Counter

Figure 1 shows the principle of ARICH counter. A photo-detector, located 20 cm away from the aerogel radiator, collects Cherenkov photons related to the passage of charged particles. PID is performed by measuring the Cherenkov angle. The angle difference between π and K for 4 GeV particle is around 23 mrad assuming the refractive index of 1.05 for the radiator. We adopted a proximity-focusing type RICH detector due to the limited available space. The number of Cherenkov photons could be increased if we used thicker aerogels, but this would have worsened the Cherenkov angle resolution due to the uncertainty of the position of Cherenkov photon emission. Therefore, we introduced two layers of 2 cm think aerogels with different indices so that the ring image overlaps at the photo-detector, which makes possible to increase the number of photons without degrading the angular resolution. We use aerogels with refractive indices of

[1] Hereafter, pions (π) and kaons (K) imply charged pions and charged kaons respectively

$n_1 = 1.045$ and $n_2 = 1.054$ and good transparency of 40 mm. The total number of aerogel tiles in ARICH is 248, and they are arranged as shown in the overview figure of ARICH (Fig. 2). Each tile has been fabricated by cutting a 18 cm $\times$ 18 cm square shape using a water jet.

The photo-detectors must be sensitive to single photons and must be capable of measuring the position with a granularity of around 5×5 mm^2. It must be immune to a 1.5 T magnetic field in Belle II, and also tolerant to the 1MeV equivalent neutron dose of 10^{12}cm^{-2} for 10-year operation. In order to fulfill these requirements, we have developed the 144-channel hybrid avalanche photo-detector (HAPD) with Hamamatsu Photonics K. K. shown in Fig. 3. The HAPD is a vacuum tube including 4 avalanche photo-diodes (APDs) in it. With the combination of the bombardment gain by high voltage ($O(1000)$) and the avalanche gain at APDs ($O(10)$), gain of around 70000 is achieved. The outer size is 73 mm $\times$ 73 mm, while effective area is 64 mm $\times$ 64 mm. The quantum efficiency at 400 mm is 28% in the specification and 32.2% in average of the HAPDs installed to ARICH. A total of 420 HAPDs are used in ARICH.

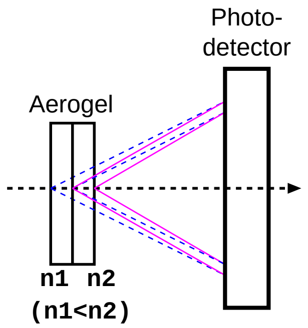

Figure 1. Principle of the ARICH counter.

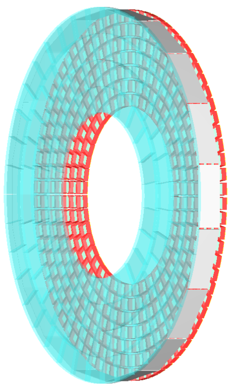

Figure 2. An overview of the ARICH detector.

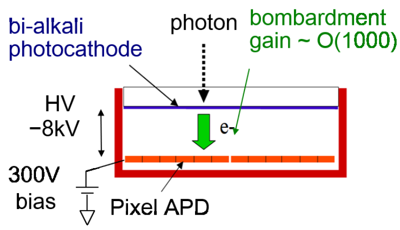

Figure 3. The structure of the HAPD.

3. Operation of the ARICH

The ARICH counter was installed to Belle II in 2017, before the Belle II commissioning run (Phase 2 run) without inner vertex detector. Then, from summer 2018, ARICH was once uninstalled for several hardware modifications including the renovation of the cooling system and repair of the malfunctioning front-end electronics. Belle II started physics run with full detector from 2019 (Phase 3 run).

Figure 4 shows the hitmap of HAPDs in a typical physics run this year. There are channels with no or few hits channels in a unit of HAPDs or APDs. A cluster of 5 dead HAPDs is due to a problem of an low-voltage cable to the front-end electronics, which will be repaired at the next chance to access the detector. A total of 3.0% of channels has problem inside APDs and bias or guard[2] voltage cannot be applied. The same problem was seen after mass production of HAPDs and for that reason some units were not installed to the ARICH. However, the number of dead APDs increased after installation, though it is getting stabilized. Another 1.7% of channels show problems with high voltage. The total dead channel fraction is now 5.9%, which has very small impact on PID performance and is acceptable.

In the high luminosity environment at SuperKEKB, large beam background is an issue for Belle II spectrometer. However, the ARICH is relatively tolerant to the beam background.

[2] An electrode to protect electric wirings from accelerated photo-electrons.

Only a small number of background hits are being measured at this moment, with a negligible contribution to the PID performance. Neutron radiation is a concern for ARICH, especially for HAPDs, because silicon bulk damage by neutrons increases the leakage current and larger noise at HAPDs. Such deterioration of the performance of HAPDs are expected during the operation of ARICH, though the effect to the PID performance is very modest with the neutron radiation up to 10^{12}cm^{-2} 1MeV equivalent neutrons, which is the expectation for 10-year operation at Belle II.

Figure 5 shows the trend of the leakage current of typical APDs in ARICH between April 2019 and May 2021. The leakage current is increasing by around 10-30 nA per month. From the irradiation test during the development of HAPDs, the increase of 30 nA corresponds to the neutron fluence of 10^9cm^{-2}. Therefore, the present estimate of neutrons at ARICH is $(0.3\text{-}1) \times 10^9\text{cm}^{-2}$ per month or $6 \times 10^9\text{cm}^{-2}$ from 2019 till May 2021. This is well below the original expectation (10^{11}cm^{-2} per year), and the neutron radiation will not be a problem in 10-year operation even if we take into account the future higher neutron dose at higher luminosity.

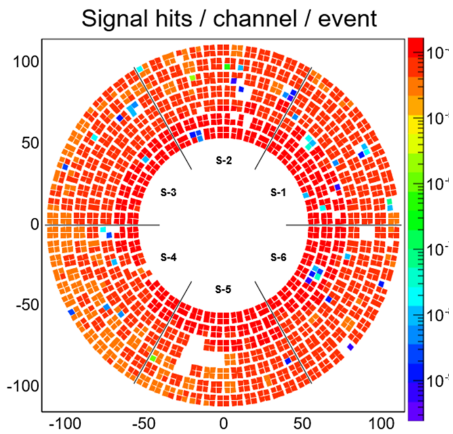

Figure 4. Typical hit distribution in ARICH. Subtraction using off-timing events is done to remove the contribution of hits not coming from the collision event. A square box in the plot corresponds to an HAPD, which is divided into 4 APDs.

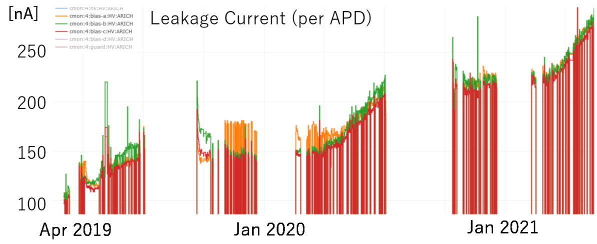

Figure 5. Leakage current per APD for a typical HAPD in ARICH.

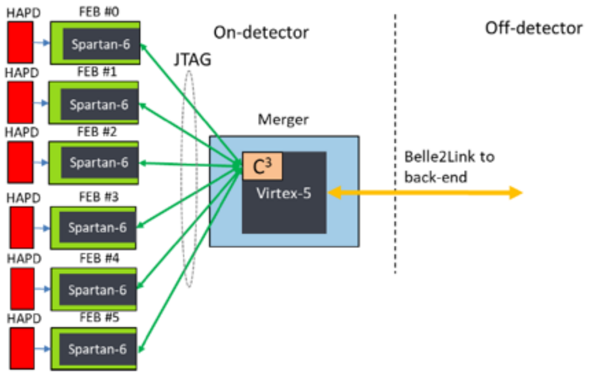

Figure 6. Overview of the readout electronics of ARICH.

Another effect that is expected from neutrons is the single event upset (SEU) in the field-programmable gate arrays (FPGAs) in the front-end electronics. Figure 6 shows the overview of the readout electronics of the ARICH. Signals from each HAPD are processed at the front-end board (FEB) attached to it. Then, the merger board located inside the ARICH detector collects data from six (or five in few cases) FEBs and sends the data to the Belle II central data acquisition system through an optical link called Belle2Link. Two kinds of FPGAs are used in the readout system of ARICH: Xilinx Spartan-6 (XC6SLX45) in FEBs and Xilinx Virtex-5 (XC5VLX50T) in mergers. Spartan-6 devices are relatively sensitive to SEUs because Boron is used as p-type dopant in the production. In our estimation based on the neutron irradiation test done in 2013, around 8 SEUs per hour per HAPD is expected in the firmware configuration memory in FEBs.

Our solution utilizes the fact that the same firmware is used in the FEBs connected to a merger. We have implemented a configuration consistency corrector (C^3) logic [3] in the merger firmware, which periodically reads frames of the firmware of FEBs through JTAG, and performs real-time bitwise majority voting on them. If some bits of the firmware from a FEB are flipped due to SEUs, a partial reconfiguration of the firmware is done for that FEB. We tested this logic in neutron irradiation tests at the TRIGA reactor of the Jožef Stefan Institute (Slovenia). Our results have shown the C^3 has better performance than the Xilinx Soft Error Mitigation IP Core, which is the solution provided by Xilinx. The logic is used in the ARICH operation from June 2020. It detects and corrects $O(0.1)$ SEUs per HAPD per day, and we observe almost no failure caused by SEUs at the Spartan 6 FPGA in FEBs during data taking at Belle II. As for Xilinx Virtex-5 FPGAs in the mergers, there have been a few DAQ failures which might be related to SEUs in that device, and this might be an issue in future high luminosity environment.

4. Performance of the ARICH

PID information by ARICH is obtained by the comparison of the hit pattern and the expected probability density function (PDF) for different particle hypothesis [4]. ARICH has only on/off hit information for each channel, and under this condition the likelihood $\mathcal{L}_h$ for a particle hypothesis is defined as

$$\ln \mathcal{L}_h = -N_h + \sum_i \left[n_{h,i} + \ln(1 - e^{n_{h,i}}) \right], \tag{1}$$

where i runs over the channel with a hit. Here, h is the particle hypothesis (e, μ, π, K, p, deuteron), N_h is the expected total number of hits, $n_{h,i}$ is the expected number of hits (i.e. probability) at pixel i for assumed particle hypothesis h. The separation of particles can be done with a likelihood ratio. For example, K/π separation is performed by applying a selection criteria on the likelihood ratio $R_{K/\pi}$

$$R_{K/\pi} = \frac{\mathcal{L}_K}{\mathcal{L}_K + \mathcal{L}_\pi}, \quad R_{\pi/K} = \frac{\mathcal{L}_\pi}{\mathcal{L}_K + \mathcal{L}_\pi} = 1 - R_{K/\pi}. \tag{2}$$

We consider the following three components in the PDF: Cherenkov photons from the aerogel, background correlated to the charged particles and random background. The first one is the signal Cherenkov peak including the photons scattered by a Rayleigh scattering inside aerogel. The second component contains the Cherenkov photons emitted inside the quartz window of HAPDs at the passage of the charged particle. The photons may also propagate inside the quartz window with total internal reflections and make a contribution to the PDF in the region of small Cherenkov angle. Cherenkov photons emitted by track-related delta rays are also included in the second component. We use different PDFs depending on whether the charged particle passes the quartz window. The random background is the background not correlated to the charged particle and includes the contribution from HAPD dark counts, electronics noise or beam background, and the contribution of this component is rather small. PDFs are calibrated with $e^+e^- \to \mu^+\mu^-$ for higher momentum particles and with $K_S^0 \to \pi^+\pi^-$ for lower momentum region.

PID performance was estimated with the sample $D^{*+} \to D^0\pi^+_{\text{slow}}$, $D^0 \to K^-\pi^+$ using the initial data taken in 2019 corresponding to 5.2 fb^{-1}. This decay is ideal for the study of kaon and pion identification (ID), because one can tell the particle species of the kaon and pion from D^0 decay using the charge of the slow pion π^+_{slow}. Figure 7 shows the distribution of D^0 mass ($K\pi$

invariant mass) after applying the D^* mass selection $|M_{D^{*+}} - M_{D^0} - 0.1454\ \text{GeV}| < 0.0015$ GeV with and without pion ID for the pions, for data and MC. Here, the target charged particle is required to be within the geometrical acceptance of ARICH. With applying the pion ID selection ($R_{\pi/K} > 0.6$), the background level becomes smaller retaining most of the signals. The obtained efficiency and mis-identification rate is summarized in Table 1. It is shown that good separation is obtained both for kaon ID and pion ID.

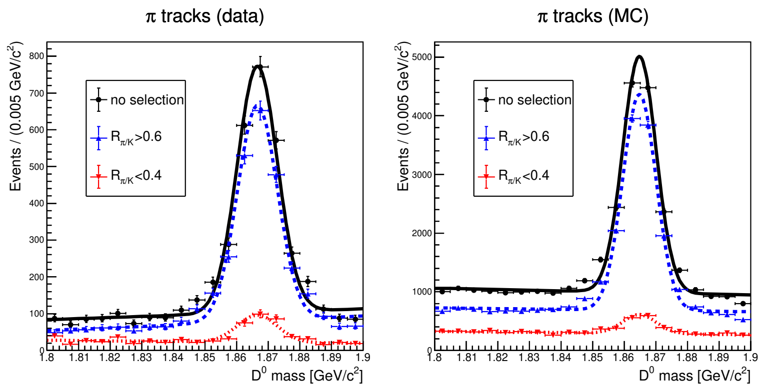

Figure 7. D^0 mass distribution in D^* sample with and without PID for data (left) and MC (right).

	Kaon ID ($R_{K/\pi} > 0.6$)		Pion ID ($R_{\pi/K} > 0.6$)	
	K eff.	π mis.	π eff.	K mis.
Data	$93.5 \pm 0.6\%$	$10.9 \pm 0.9\%$	$87.5 \pm 0.9\%$	$5.6 \pm 0.3\%$
MC	$96.7 \pm 0.2\%$	$7.9 \pm 0.4\%$	$91.3 \pm 0.3\%$	$3.4 \pm 0.4\%$

Table 1. PID performance of ARICH obtained from D^* control sample. Eff. (mis.) means efficiency (mis-identification).

More effort is going on to improve the PID performance. Improvement of the PDFs by implementing minor structure of the Cherenkov ring image, such as the reflection of the Cherenkov light inside HAPDs, is under study and is promising to improve the PID performance. Another observation is that mis-identification partly comes from the decay or hard scattering of the charged particles. In such a case, particles do not arrive at ARICH and they tend to be mis-identified as kaons. This is why kaon ID has larger mis-identification rate than pion ID in Table 1, and possible identification of such particles using the information of the calorimeter behind ARICH is under trial.

5. Conclusion

ARICH, a proximity focusing RICH detector with aerogel radiator, is under successful operation as a PID device in the forward endcap at Belle II. Damage of HAPDs by neutrons are anticipated for 10-year operation, but the neutron fluence is well below the tolerable level. The initial performance of ARICH is estimated and good PID performance is obtained. Further improvement of the performance is expected.

References

[1] T. Abe *et al.* (Belle II Collaboration), "Belle II Technical Design Report," arXiv:1011.0352 [physics.ins-det].
[2] Y. Ohnishi *et al.*, PTEP **2013**, 03A011.
[3] R. Giordano *et al.*, arXiv:2010.16194 [physics.ins-det].
[4] M. Yonenaga, *et al.*, PTEP **2020**, 093H01.